https://doi.org/10.5194/egusphere-2025-2357
Preprint. Discussion started: 2 June 2025

Coastal Nitrogen Drives Respiration Quotient in the Southern California Bight

Allison R. Moreno[1,2], Adam J. Fagan[3], and Adam C. Martiny[2,3]

Affiliations:
[1] Department of Ocean Sciences, University of California, Santa Cruz, CA, USA
[2] Department of Ecology and Evolutionary Biology, University of California, Irvine, CA, USA
[3] Department of Earth System Science, University of California, Irvine, CA, USA
Correspondence to: Allison R. Moreno (amoren53@ucsc.edu)

Abstract. Southern California Bight coastal waters are dynamic and strongly influenced by a changing climate. An increased respiration quotient has been found during high temperature and low nitrogen conditions. These observations are specific to open ocean conditions, and their applicability to coastal environments is uncertain. To disentangle the controlling factors in a coastal environment, we examined environmental conditions, particulate organic matter, and the respiration quotient over five years in the Southern California Bight. Our study revealed clear seasonal variation in environmental conditions and biological parameters. We detected higher than previously reported respiration quotient ratios in open ocean regions. We found a strong inverse relationship between respiration quotient, nitrate and chlorophyll. Our findings also suggest that changes in community structure, triggered by nutrient shifts and a local oil spill, affected the range in respiration quotient and explains some of the variability measured. As climate continues to impact coastal regions, variable $r_{O2:C}$ patterns and its controls assists in accessing subsurface oxygen concentrations and in turn the health of our coastline.

1. Introduction

Oxygen is vital for coastal ecosystem health, acting as the primary oxidizing agent in cellular respiration. Along the eastern California Current, increased upwelling, mixing, and remineralization rates result in higher nutrient availability during winter and spring months (Venrick 2012), driving seasonality in dissolved oxygen throughout the water column (Bograd et al. 2008). Coastal deoxygenation events have been found to be primarily driven by nutrient cycling (Falkowski et al. 2011; Schmidtko et al. 2017). The respiration quotient, the amount of oxygen required for full carbon oxidation, $r_{O2:C,}$ is a direct measurement that can help to assess future changes in oxygen. The respiration quotient has been linked to changes in surface plankton community composition and may express changes in deep oxygen through bacterial consumption (Moreno et al. 2020). Additionally, the amount of exported organic carbon and associated oxygen consumption due to bacterial respiration is sensitive to temperature and has a strong impact on oxygen levels (Matear and Hirst 2003; Keeling et al. 2010). As expected globally, temperatures will continue to rise in the Pacific Ocean, slowly warming the California coastline despite seasonal upwelling. However, the respiration quotient has not been quantified in coastal waters to date. Consequently, it is critical to quantify coastal $r_{O2:C}$ patterns to determine which environmental factor controls its variation and hypothesize future shifts in oxygen levels.

Open ocean $r_{O2:C}$ varies systematically with temperature and nutrients to produce distinct basin patterns. $r_{O2:C}$ has been shown to vary positively with temperature along the Eastern Pacific Ocean (Moreno et al. 2020) and in nitrogen limited regions in the Atlantic Ocean (Moreno et al. 2022). Increased $r_{O2:C}$ is representative of larger oxygen consumption by bacteria or higher trophic organisms during respiration. Regions with high temperatures and deep nutriclines were found to have high $r_{O2:C}$ ratios in the Pacific Ocean (Moreno et al. 2020). Further, nitrogen stress caused increased $r_{O2:C}$ resulting in ratios higher than with temperature alone. In contrast, phosphorus stress appeared to dampen ratios, particularly when combined with high temperatures (Moreno et al. 2022). Beyond the mixed layer, $r_{O2:C}$ decreased to its minimum at the euphotic and disphotic boundary (Gerace et al. 2023). It was hypothesized that planktonic community structure and the preferential production/removal of biochemical components (i.e.,

https://doi.org/10.5194/egusphere-2025-2357
Preprint. Discussion started: 2 June 2025

lipid followed by proteins) led to a steady decrease in $r_{O2:C}$ (Gerace et al. 2023). However, from the base of the euphotic zone to depth, the $r_{O2:C}$ remained relatively consistent with the average higher than the mixed layer. Oxygen consumption was consistent, resulting in an overall decrease in the deep oxygen concentrations. Thus, systematic relationships exist with environmental conditions in the open ocean and provide evidence for coastal variation.

The Southern California Bight (SCB) is ever dynamic and changing due to climatic influences creating a unique study site. Previous work, at the 'Microbes in the Coastal Region of Orange County' (MICRO) time-series, quantified variation in the particulate organic matter (POM) concentrations and stoichiometric ratios corresponded to seasonal and multi-year oscillations in environmental conditions and phytoplankton abundances (Martiny et al. 2016; Fagan et al. 2019, p. 20; Larkin et al. 2020). Specifically, high C:N:P corresponded to summer/fall periods with high temperatures, low nutrients and a small phytoplankton dominance and vice versa for cooler periods during the winter and spring. Harmful algal bloom (HAB) forming species are present year-round, range in size and play a significant role in SCB biogeochemical cycling (Trainer et al. 2010). Changes in bloom behavior due to natural or anthropogenic influences will influence POM concentrations and stoichiometric ratios. As such, we expect $r_{O2:C}$ to exhibit seasonality and follow previously quantified stoichiometric ratio patterns with increased values during warm, low nutrient seasons, as well as major variation due to bloom formation and/or shifts in community structure.

In October 2021, an oil spill deposited over 20,000 gallons of crude oil onto Southern California beaches creating a natural community shift experiment. Many studies have found a high presence of hydrocarbon degrading bacteria during oil spills, shifting the microbial community structure away from seasonality (Hazen et al. 2010; Yang et al. 2014). Their magnitude is closely related to the season and type of oil during the event (Fuentes et al. 2016; Varjani and Gnansounou 2017). As a result, the bulk particulate matter (i.e. surface plankton community) will shift while oil persists in the water column and could cause a lag in seasonal community composition from pre-oil conditions. It has been hypothesized that changes to the bulk carbon type could alter the $r_{O2:C}$ average ratio (Moreno et al. 2020). Provided with this unique opportunity affecting our study site, we expect to quantify increased $r_{O2:C}$ patterns while oil is present and possible shifts from seasonal or annual patterns.

The goal of this study was to quantify $r_{O2:C}$ and identify possible drivers of its coastal temporal dynamics. To this end, we quantified changes in temperature, nutrients, POM concentrations and $r_{O2:C}$ ratios at the MICRO time-series in the SCB weekly from October 2016 to January 2022. We predicted that the cumulative average $r_{O2:C}$ will be higher than previously quantified open ocean ratios due to increased coastal dynamics and higher anthropogenic influence. We also predicted observing seasonal patterns in $r_{O2:C}$, strongly controlled by temperature rather than changing in nutrient stress. As planktonic community composition shifts from larger to smaller species, we anticipated $r_{O2:C}$ will increase. Finally, we expected that increased complex hydrocarbons during the oil spill period will decrease $r_{O2:C}$ ratios.

2. Material and Methods

2.1. Seawater Collection

Surface water was collected weekly at the MICRO time-series study site (33.608˚N and 117.928˚W; Martiny et al. 2016). Two autoclaved bottles are rinsed with ocean water and filled for processing in the lab. Water temperature and chlorophyll a data are collected from an automated shore station off Newport Pier as part of the Southern California Coastal Ocean Observing Systems (SCCOOS).

Triplicate 300 ml samples for particulate organic carbon (POC) and particulate chemical oxygen demand (PCOD) from each bottle are filtered within an hour of collection through pre-combusted (500˚C, 5 hr.) 25 mm GF/F filters (Whatman, MA). Each filter is rinsed with Milli-Q water before sample filtration to remove potential P residues. Filters are stored in a starred petri dish. POC samples were placed directly into the -20˚C freezer. The PCOD samples are dried for 24 hr. at 55˚C and then placed in the -20˚C freezer. The filtrate from the initial filtration is collected and used for macronutrient

https://doi.org/10.5194/egusphere-2025-2357
Preprint. Discussion started: 2 June 2025

quantification. The filtrate is filtered through a 0.2 µm syringe filter into a 50 ml tube. Triplicates were taken for nitrate and phosphate and stored in the -20˚C freezer.

2.2. Macronutrients Quantification

Soluble reactive phosphorus (SRP) concentrations were determined using the magnesium induced co-precipitation (MAGIC) protocol and calculated against a potassium monobasic phosphate standard (Karl and Tien 1992; Lomas et al. 2010). Nitrate samples (taken before 2019) were treated with a solution of ethylenediaminetetraccetate and passed through a column of copperized cadmium fillings (Knap et al. 1993). Nitrate samples (taken after 2019) were measured using a spongy cadmium method (Jones 1984).

2.3. Particulate Organic Carbon (POC)

After thawing, POC filters were allowed to dry overnight at 65˚C before being packed into a 25 mm tin capsule (CE Elantech, Lakewood, New Jersey). Samples were then analyzed for C content on the FlashEA 112 nitrogen and carbon analyzer (Therom Scientific, Waltham, Massachusetts), following the Sharp (1974) protocol. POC concentrations were calibrated using known quantities of atropine ($C_{17}H_{23}NO_3$) and acetanilide (C_8H_9NO).

2.4. Particulate Chemical Oxygen Demand (PCOD) Assay

PCOD samples were quantified following Moreno (2020). Samples were placed in 50˚C for 24 hr. Filters were then transferred to HACH HR+ COD vials (Product no. 2415915 containing mercuric sulfate). Two mL of Milli-Q water was added to each vial and inverted to submerge the filers completely. Vials are digested at 150˚C for 2 hr. in a digestion block. Samples were then cooled to room temperature. Due to uneven precipitation occurring, precipitation was induced by adding 92.1µL of 0.17M (or 9.5g L^{-1}) NaCl to each vial. Vials were inverted twice and centrifuged for 30 minutes at 2500 rpm and read on a photo-spectrometer at a wavelength of 600 nm. Note: Dichromate does not oxidize organic nitrogen, so this assay only quantifies changes in the carbon oxidation state. To quantify PCOD, in µM O_2, we utilize a standard curve based on HACH certified COD 1000 mg/L standard stock solution (Product no. 2253929).

2.5. $r_{O2:C}$ Ratio

$r_{O2:C}$ ratios were taken from the mean concentrations of PCOD and POC triplets. We compare our measured $r_{O2:C}$ ratio to that of Redfield (1; Redfield 1958) and Anderson's best estimate average cell value of 1.1 (Anderson 1995). The standard deviation for $r_{O2:C}$ were calculated as a pooled sample:

$$\sigma_{\mathrm{r-O2:C}} = \frac{-O_{2,aver}}{C_{aver}} \times \sqrt{\left(\left(\frac{\sigma_{-O2}}{-O_{2,aver}}\right)^2 + \left(\frac{\sigma_C}{C_{aver}}\right)^2\right)}$$

2.6. Large Phytoplankton Relative Abundance

Phytoplankton abundance for ten species, two general species categories and the total phytoplankton abundance were obtained from SCCOOS. Water collection and analysis can be found at (Seubert et al. 2013). The ten species are as follows: *Akashiwo sanguinea, Alexandrium spp., Dinophysis spp., Lingulodinium polyedra, Prorocentrum spp., Pseudo-nitzschia (PN) delicatissima, PN seriata, Ceratium spp., Cochlodinium spp.,* and *Gymnodinium spp.* The two categories are 'Other Diatoms' and 'Other Dinoflagellates' (Table 1). Monthly and annual average relative abundance were calculated by averaging the abundance for each species over the specific time span (either monthly or annually) then dividing by the total abundance for that same period.

2.7. Statistical Analysis

All analyses were done using Table S1 data in Matlab (Mathworks, MA). Using the smooth function, a four-point or eight-point moving average was overlaid onto the raw data time-series plots. Sum of square analysis was conducted on linear regressions to quantify the monthly and annual

https://doi.org/10.5194/egusphere-2025-2357
Preprint. Discussion started: 2 June 2025

contributions. To detrend seasonality in our time-series parameters, we apply a season adjustment using a stable seasonal filter applying a 53-point moving average, representing our weekly sampling. To determine potential covariations, a Pearson's correlation coefficient was calculated for each pair of environmental variables, followed by a test of statistical significance (p-value ≤ 0.05). Similarly, a Pearson's correlation coefficient was calculated between each species abundance and chlorophyll, followed by a statistical significance (p-value ≤ 0.05) test, to determine which species influenced chlorophyll concentrations.

To determine impacts on $r_{\text{-}O2:C,}$ a Pearson's correlation coefficient was calculated for each pair of species relative abundance and $r_{\text{-}O2:C,}$ followed by a statistical significance test (p-value ≤ 0.05). Due to limited data in the large phytoplankton relative abundance, we removed *Ceratium spp., Cochlodinium spp.,* and *Gymnodinium spp*. from the annual correlation analysis.

Statistical nonlinear models were fitted using six predictor variables (temperature (˚C), nitrate (µM), phosphate (µM), chlorophyll (mg C/m^3), POC (µM), and PCOD (µM)). R^2 and Akaike Information Criterion (AIC) were used to compare across models. For all regressions containing interpolated parameters, a random sampling of cruise data was conducted to ensure results were not swayed.

Oil spill analysis was accomplished using a 2-way ANOVA. First $r_{\text{-}O2:C}$ ratios were averaged over three months before the spill (July through September), the month during the spill (October), and three months after (November through January) during 2021/2022. Similar averaging was done for 2018/2019 and 2019/2020 years to quantify differences between the average $r_{\text{-}O2:C}$ ratios during this period and specifically during the oil spill.

3. Results

To evaluate our hypothesis that $r_{\text{-}O2:C}$ demonstrates seasonal variability, and has systematic relationships with temperature and nutrient availability, we quantified physical (temperature), chemical (nitrate and phosphate), and biological [chlorophyll, particulate organic carbon (POC) and particulate chemical oxygen demand (PCOD)] properties and stoichiometric ratio ($r_{\text{-}O2:C}$) over a 5-yr period from 2016 to 2022. Annual oscillations and strong correlations exist between parameters.

3.1. Temporal Patterns

Physical conditions demonstrate short-term, seasonal, and annual trends. As expected for a site at 33˚N, temperature oscillated annually with a peak in August and trough in January (Fig. 1A). The highest average temperature occurred in 2018 with an annual mean of 18.05˚C. As described previously, nutrient availability showed a strong seasonal anti-correlation with temperature (Martiny et al. 2016; Fagan et al. 2019) as well as clear monthly and annual differences (Fig. S1). Temperature correlations are highly dynamic on weekly, monthly, and annual timescales (Fig. S2). Temperature dynamics covaried with macronutrients. Macronutrient concentrations demonstrate clear patterns. Phosphate concentrations appeared to have a 3-year systematic shift, going from approximately 0.2 µM and steadily increasing to approximately 0.6 µM (Fig. 1B). This pattern was seen from 2016 to 2019, and again from 2019 to 2022, with a quick drawdown occurring winter 2018/2019 corresponding to an increase in chlorophyll. Phosphate was highest during the winter months, and lowest during the late summer. Weekly phosphate was correlated with temperature and nitrate (Fig. S3A). Nitrate concentrations shift on annual and seasonal cycles (Fig. 1C). Generally, nitrate was highest (with the least amount of variation) in 2018 and lowest (with the highest variation) in 2022 (Fig. S1). Nitrate was correlated with weekly temperature, phosphate, and $r_{\text{-}O2:C}$ (Fig. S2A). Nitrate and phosphate, on monthly scales, were correlated with each other, and temperature (Fig. S2B). In late 2017 to 2019, nitrate and phosphate were consistently higher than during the late 2019 to 2021 timeframe. Chlorophyll follows a seasonal cycle with peaks during period of low nutrients, possibly responding their drawdown of nutrients for growth. Dynamic

https://doi.org/10.5194/egusphere-2025-2357
Preprint. Discussion started: 2 June 2025

environmental conditions at MICRO could have strong impacts on biological parameters leading to distinct patterns.

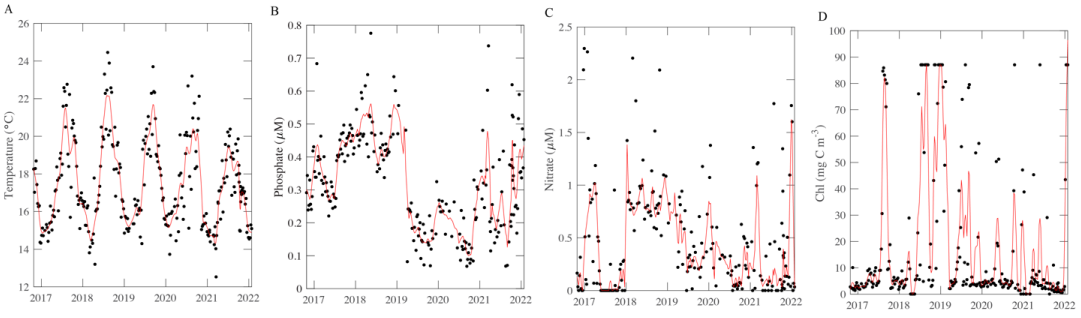

Figure 1. Environmental conditions, macronutrient, and chlorophyll concentrations (A- D) over time at MICRO study site in Newport Pier, Newport, CA. The solid black points represent the average data per week from the period 10/26/2016 to 1/31/2022. The red line represents an 8-point moving average.

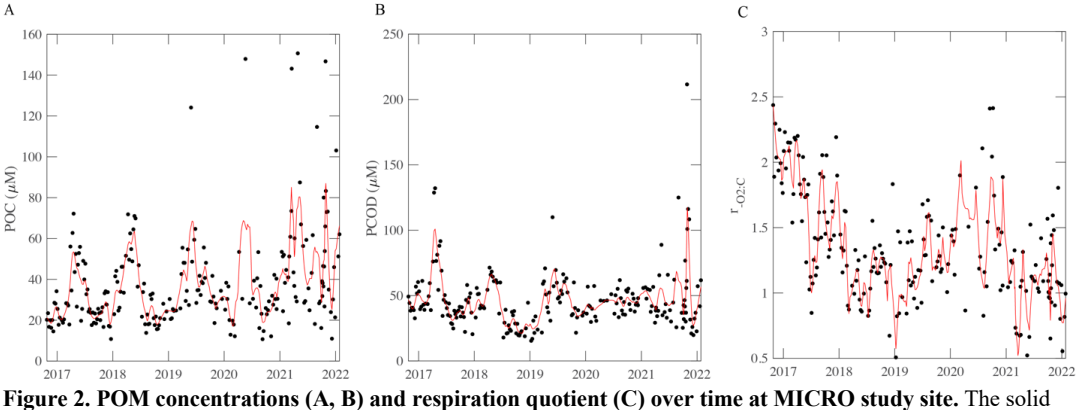

Figure 2. POM concentrations (A, B) and respiration quotient (C) over time at MICRO study site. The solid black points represent the average data per week from the period 10/26/2016 to 1/31/2022. The red line represents a 12-point moving average. The respiration quotient is a molar ratio.

POM parameters also demonstrated short-term, seasonal and annual variation. [POC] and [PCOD] concentrations peaked during the spring bloom period (May) and oscillated annually (Fig. 2A, B and Fig. S1, S2). Generally, [POC] had similar variability to [PCOD] (p-value < 0.05; Fig. 2A, B). [POC] appeared to be increasing through time with the highest annual average occurring in 2022. [POC] correlated with physical conditions (Fig. S2). [PCOD] was significantly higher in April and May (Fig. S1). [PCOD] also had its highest annual average in 2022. Annually [PCOD] covaried with temperature (Fig. S2C). However, where [POC] was lowest in 2020, [PCOD] had a minimum in 2018 (Fig. S2). Overall, biological parameters showed similar multiannual oscillations as environmental conditions, indicating consistency between the two.

3.2. Coastal $r_{O2:C}$ ratios

The respiration quotient showed clear temporal variation, but no significant seasonality was found. The average $r_{O2:C}$ ratio was 1.34, which was statistically higher (t-test, p-value < 0.05) than Redfield (1), Anderson (1.1), and previous open ocean estimates (1.16; Moreno et al. 2022). Although the average was higher, the range in values was smaller compared to open ocean samples. Generally, the highest monthly $r_{O2:C}$ were found in February and September (Fig. S3). However, the highest weekly $r_{O2:C}$

https://doi.org/10.5194/egusphere-2025-2357
Preprint. Discussion started: 2 June 2025

$r_{O2:C}$ peak occurred in January and into February 2020, while [POC] values were low (Fig. 2C). The lowest average annual $r_{O2:C}$ (0.99) was measured in 2022. Additionally, a multi-year (~3 year) trend was detected whereby $r_{O2:C}$ decreased from 2016 to 2020 and concentrations peak at 1.85 (Fig. 2C). Weekly nitrate and [POC] were found to correlated with changing $r_{O2:C}$ (Fig. S3). We found distinct variation in the respiration quotient ratio at the MICRO site.

We assessed environmental changes using a multi-dimensional principal component analysis (Fig. 3). As shown above, changes in environmental conditions can covary and be associated with changes in particulate organic matter (Fig. S2). We explicitly accounted for this co-variance using principal components (PC) and linked each PC to $r_{O2:C}$ variation. Our PC analysis explained ~81% of the $r_{O2:C}$ variance. The environmental parameters used within the multi-dimensional analysis were temperature, phosphate, nitrate, and chlorophyll concentrations. Our first principal component (PC1) represented blooming conditions (i.e., positive chlorophyll) representing 50% of overall variance. PC2 captured the environmental axis, dominated by seasonality (~31%; Fig. 3). Thus, PC2 corresponded to a decreased temperature and increased nutrient concentration. Specifically, high $r_{O2:C}$ ratios can be found under low nitrate and chlorophyll concentrations. Similar to open ocean analysis, when only considering a single environmental parameter, nitrate concentrations control $r_{O2:C}$ such that increased $r_{O2:C}$ is present during nitrogen stress (p-value = 0.0207, r^2 = 0.023). Our analysis demonstrated an anti-correlation with environmental conditions which suggests that higher $r_{O2:C}$ is present under high temperature and low nutrient conditions. This corresponds to blooming behavior- as nutrients stimulate bloom formation $r_{O2:C}$ was low, and as blooms dissipate the $r_{O2:C}$ increased. $r_{O2:C}$ is shifting based on the environmental impacts on community composition.

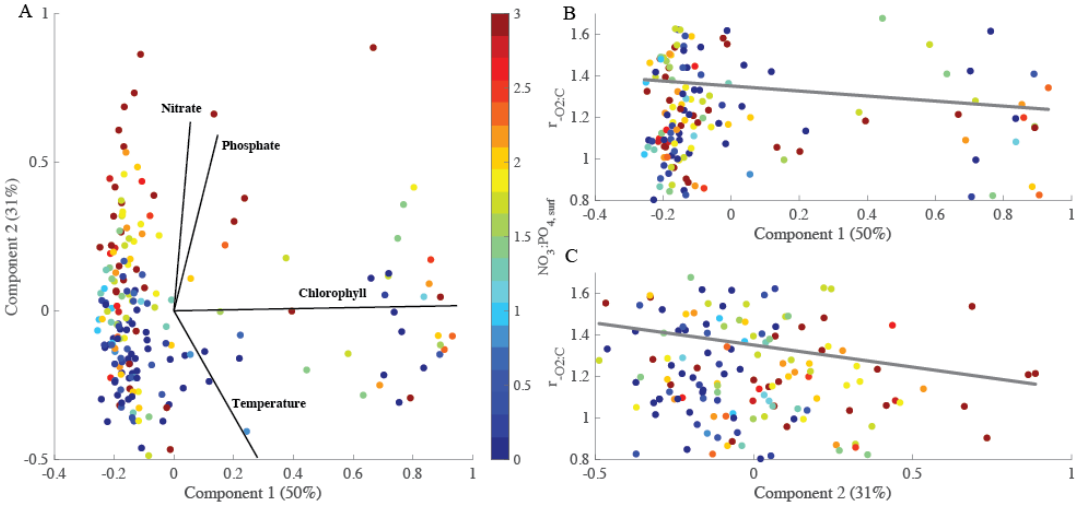

Figure 3. PCA analysis of $r_{O2:C}$ to determine the overall controlling factors. A. PCA of four environmental variables (nitrate concentrations, phosphate concentrations, chlorophyll concentrations, and temperature) over 5-years at the MICRO site. B. and C. $r_{O2:C}$ explained by the first and second principal component including the $r_{O2:C}$ based on linear regression analysis. The percentages of total variance represented by principal component (PC) 1 and 2 are shown in parentheses. Colored dots represent the NO_3:$PO_{4,\ surf}$ concentration. Grey solid lines represent regression lines with r^2 = 0.0003 (B) and 0.012 (C).

3.3. Large Phytoplankton Abundance

Large harmful algal bloom (HAB) phytoplankton abundance demonstrated clear shifts over the time-series. California experienced seasonal and environmentally driven HAB blooms. Ten HAB species and two categories of large phytoplankton (Table 1) were quantified and compared over our time-series to determine if community structure plays a role in $r_{O2:C}$ variation. Seasonal cycling can be observed in

https://doi.org/10.5194/egusphere-2025-2357
Preprint. Discussion started: 2 June 2025

Prorocentrum, *Pseudo-nitzschia (PN) delicatissima*, *PN seriata*, 'Other Diatoms', and 'Other Dinoflagellates' (Fig. S4). Whereas other species, i.e. *Akashiwo*, *Alexandrium*, *Cochlodinium* and *Gymnodinium*, are observed sparingly. On weekly timescales, *Akashiwo* had a positive relationship with chlorophyll a concentration (p-value = 0.004, r = 0.03), whereas 'Other Dinoflagellates" has a negative relationship (p-value = 0.032, r = -0.02). On monthly timescales, the 'Other Diatoms' and 'Other Dinoflagellates' made up 50 to 80% of total phytoplankton (Fig. 4A). Following this majority, we observed significant concentrations of *Prorocentrum*, *PN delicatissima* and *PN seriata*. During typical blooms months (spring and August) we estimated a higher presence of species, with an increase in a few species during these months. Similarly, annual relative phytoplankton abundance observations were highly dominated by 'Other Diatoms' and 'Other Dinoflagellates' (Fig. 4B). *Akashiwo*, *Alexandrium*, and *Dinophysis* were found in very low concentration throughout the time-series, however, evidence shows their impact could be great even so. Species sampling was paused from March to June 2020, which may explain the lowest diversity compared with other years. In 2021, the 'Other' categories were at their lowest at 40% of the total phytoplankton present. Additionally, in 2021 and 2022, *Lingulodinium*'s relative abundance becomes a significant part of the breakdown at approximately 15 to 20%. Accordingly, we observed clear shifts in the phytoplankton community composition and corresponding relative abundance of larger cell volume species over our time-series.

Table 1. Quantified genius and category of large harmful algal bloom phytoplankton.

Type	Genius/Species	Size Range
Dinoflagellates	*Akashiwo sanguinea*	40 – 80 µm
Dinoflagellates	*Alexandrium spp.*	20 – 80 µm
Dinoflagellates	*Dinophysis spp.*	35 – 50 µm
Dinoflagellates	*Lingulodinium polyedra*	40 – 54 µm
Dinoflagellates	*Prorocentrum spp.*	40 – 50 µm
Diatoms	*Pseudo-nitzschia delicatissima*	40 – 80 µm
Diatoms	*Pseudo-nitzschia seriata*	105 - 115 µm
Dinoflagellates	*Ceratium spp.*	20 – 200 µm
Dinoflagellates	*Cochlorinium spp.*	30 – 50 µm
Dinoflagellates	*Gymnodinium spp.*	40 – 75 µm
Diatoms	'Other Diatoms'	20 – 200 µm
Dinoflagellates	'Other Dinoflagellates'	5 – 2,000 µm

Shifts in community structure impact $r_{\text{-}O2:C}$ patterns. Akashiwo sanguinea, on a weekly basis, was found to positively correlate with $r_{\text{-}O2:C}$ (r = 0.18, p-value <0.05) and 'Other Dinoflagellates' were found to have a negative relationship (r = - 0.14, p-value <0.05). Mean $r_{\text{-}O2:C}$ is associated with months that contain more diverse relative abundance in large phytoplankton (January, April, and August; Fig. S3 and Fig. 4). In March and May, 'Other Diatoms' and 'Other Dinoflagellates' reduce in abundance, and this correlated to months with the lowest $r_{\text{-}O2:C}$. Comparatively, during these months *Pseudo-nitzschia* species are in highest relative abundance. This result is expected as upwelling replaces the surface with cooler nutrient rich waters stimulating plankton growth. In January, *Akashiwo sanguinea* is present in observable concentrations and associated with lower $r_{\text{-}O2:C}$ (Fig.4 and Fig. S5A). *Akashiwo sanguinea* are similar in size to *Pseudo-nitzschia delicatissima*, which may provide evidence of a relationship between cell size and variation in $r_{\text{-}O2:C.}$. We found additional general trends which provide a possible line of evidence for future work (Fig. S5B). In 2016 and 2020, the relative abundance of 'Other Diatoms' and 'Other Dinoflagellates' is approximately 80% and was associated with high $r_{\text{-}O2:C}$ values (Fig. 4 and Fig. S3). However, in years with high distinct diversity (2019 and 2021), where 'Other Diatoms' and 'Other Dinoflagellates' relative abundance is low, the average $r_{\text{-}O2:C}$ is low (Fig. 4). As such, we demonstrate that community structure shifts can play a role in the average $r_{\text{-}O2:C}$ and its variability.

https://doi.org/10.5194/egusphere-2025-2357
Preprint. Discussion started: 2 June 2025

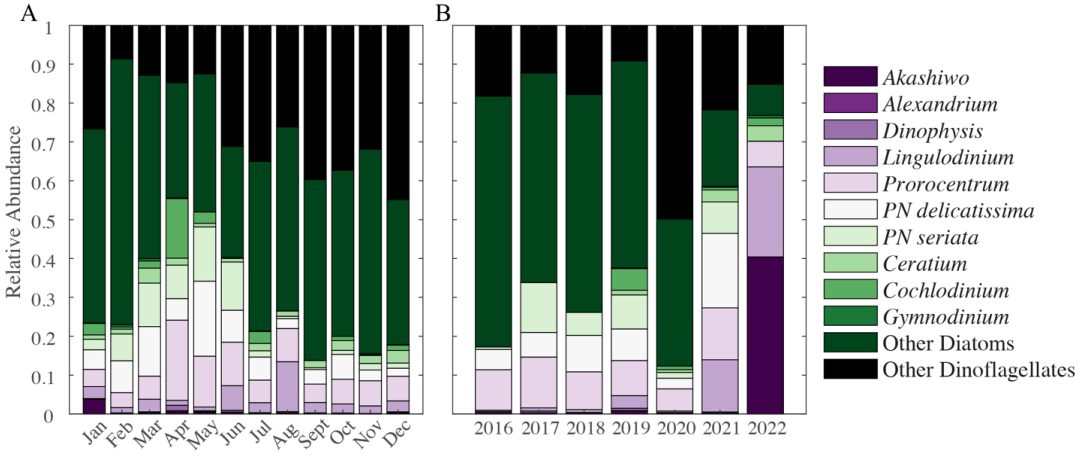

Figure 4. Monthly (A) and annual (B) large phytoplankton relative abundance. Each color represents a different species, genus, or category of diatom or dinoflagellate.

3.4. Orange County 2021 Oil Spill

The oil spill event had an impact on $r_{\text{-}O2:C}$ ratios. There was no immediate response in $r_{\text{-}O2:C}$ to the oil spill following the first day of its occurrence (Fig. 5). However, in the following days (approximately a 2-day later), an increase in the [POC] and [PCOD] persisted until the beginning of November. However, there is a slight discrepancy between [POC] and [PCOD] in the first few November measurements (Fig. 5). [POC] continued to peak in the first week before starting to come down, whereas [PCOD] started to decrease immediately. $r_{\text{-}O2:C}$ show similar trends- increases after a 2-day lag. $r_{\text{-}O2:C}$ recovery is complicated to quantify; however, it appears that values are slightly lower but within range of pre-oil spill concentrations. Statistically, there is no difference in average $r_{\text{-}O2:C}$ between 3-months before, 1-month while oil was present in samples (during), and 3-month after. Intriguingly, when compared with other years (2019, 2020, and 2021), the 2021 oil spill year did have overall lower $r_{\text{-}O2:C}$ averages (Fig. S6). $r_{\text{-}O2:C}$ in 2020 has the highest concentrations for this comparative period. However, due to the range within the time periods, there is no statistical annual differences. Thus, the oil spill does appear to influence $r_{\text{-}O2:C}$ variability, though more research is needed to fully disentangle the mechanistic controls.

https://doi.org/10.5194/egusphere-2025-2357
Preprint. Discussion started: 2 June 2025

Figure 5. Biological parameters (A. POC, B. PCOD, and C. $r_{O2:C}$) from July 1, 2021, to January 31, 2022. This represents a 3-months before to 3-months after the oil spill occurrence. The red line represents an 8-point moving average. The red star marks the start of the oil spill.

4. Discussion

We find evidence that nutrient limitation controls the $r_{O2:C}$ patterns in the coastal MICRO study site. Within this dynamic location, we have quantified a larger average in this ratio ($1.34^{2.43}_{0.51}$) compared to open ocean samples ($1.16^{1.93}_{0.75}$; Moreno et al. 2022). Temperature and nutrient availability are the two main environmental controls that have been shown to influence the respiration quotient in surface open ocean communities (Moreno et al. 2020, 2022). Direct quantifications of environmental parameters, large HAB forming phytoplankton relative abundance, and the $r_{O2:C}$ allowed us to disentangle patterns and hypotheses to determine the relative control of abiotic vs. biotic processes in a coastal setting. At the MICRO site, we find that low nitrate and chlorophyll concentrations correspond to higher [PCOD] and in turn higher $r_{O2:C}$ (Fig. 1 and 2). Higher N stress can decrease productivity and therefore lower chlorophyll concentrations. Under N stress many microalgae will increase their lipid content (Thompson et al. 1992; Reitan et al. 1994; Juneja et al. 2013) in turn increasing their average $r_{O2:C}$. This is one line of evidence to explain our findings. Another possibility is samples only capture a snapshot of the community structure. Changes in nutrients in this highly dynamic location will result in a plankton dominance shift affecting the possible chlorophyll concentration. Our results indicate an interaction between N stress and chlorophyll a, which corresponds to a response in $r_{O2:C}$.

We also have strong evidence that $r_{O2:C}$ is also directly influenced by the community structure. There are connections between $r_{O2:C}$ and the large phytoplankton relative abundance (Fig. 4). On monthly time scales, the relative abundance closely follows nitrate concentrations (Fig. S1C). Previous time-series studies of cyanobacteria have demonstrated interannual patterns in ecotype relative abundance and seasonal switching in ecotype occurring in response to rapid environmental changes (Tai and Palenik 2009; Malmstrom et al. 2010; Nagarkar et al. 2018). Although we do not quantify cyanobacteria in this study, previous published work at the MICRO site with a short overlapping window agrees with an ecotype shift being captured (Larkin et al. 2020). *Prochlorococcus* HLI dominate the cyanobacterial community under high temperature and lower nitrate concentration, whereas *Synechococcus* IV dominate in lower temperatures and higher nitrate. Utilizing our hypotheses, we expect that under high temperature and N limitation, $r_{O2:C}$ would be relatively high. Our 2016 to 2018, $r_{O2:C}$ ratios overlap with the Larkin data (Fig. 4) and as expected $r_{O2:C}$ is highest in 2016 when *Prochlorococcus* HLI is in highest abundance. As *Synechococcus* IV dominates the region, the $r_{O2:C}$ ratio decreases. Others have suggested that midwater microbial communities are vital to understanding ocean deoxygenation and its influence on decreasing oxygen concentration (Robinson 2019). Overall, we find evidence that a shift in phytoplankton communities particularly due to a change in nutrient availability will increase the range in $r_{O2:C}$ ratios.

Crude oil does not directly affect $r_{O2:C}$ ratios but appears to indirectly affect the community dominance. $r_{O2:C}$ do not show a significant impact compared with a three-month period before and after (Fig. 5 and Fig. S5). Instead, a two-day lag in $r_{O2:C}$ ratios exist (Fig. 5), which could be attributed to a community response to the amount and type of oil present. Hydrocarbon degrading bacteria are always present in small concentrations in most coastal regions, especially in highly anthropogenically impacted coastlines. Incubation experiments found large significant shifts in both bacterial and archaeal communities in seawater (Aktas et al. 2013). After the initial oil spill day, our [PCOD] and [POC] increased resulting in a slight $r_{O2:C}$ increase. This response could be due to the continued increase in oil concentrations and its effect on the community. Increased oil can preferentially cause certain bacterial and archaeal species to bloom and affect the rate of degradation- some compounds will degrade quickly and others extremely slowly (Leahy and Colwell 1990). As the oil is degraded to low concentrations (or background values in our coastal setting), $r_{O2:C}$ ratios taper off to normal values and behaviors. Although $r_{O2:C}$ does not show large shifts during the oil spill, there is evidence that oil presence does indirectly impact $r_{O2:C}$ ratios through community shifts and their physiological responses.

https://doi.org/10.5194/egusphere-2025-2357
Preprint. Discussion started: 2 June 2025

There are multiple caveats to be considered within this study that could affect the overall findings. The most prominent and obvious is the extremely high respiration quotient ratios. We quantify ratios that are higher than previously measured and expected. Within our data, higher ratios typically corresponded to higher [PCOD] rather than a lower [POC]. One possibility that needs to be explored in the future is if our [PCOD] assay is capturing the oxidation of iron (Fe) and/or biogenic sulfur (S) on samples. Trace concentrations of either would be difficult to explicitly quantify from samples taken. Dissolved Fe is a main limiting nutrient along the California Current system (Hutchins et al. 1998). However, iron from continent margin sediments have been shown to affect primary production and carbon export in the Pacific Ocean (Johnson et al. 1999; Lam et al. 2006). A small fraction of the sediment-derived Fe remains in solution as organic ligands (Kondo and Moffett 2015; Homoky et al. 2021) or in suspension as colloids or nanoparticles (Pan et al. 2011; Krachler et al. 2012). Sulfur, on the other hand, makes up about 1% of organismal dry weight and is rarely limited in the ocean. There is a large variation in its oxidation state, ranging from completely reduced (-2) to completely oxidized (+6). Inorganic sulfur compounds thiosulfate and sulfite can be transformed to hydrogen sulfide and sulfate by bacteria making these S species readily available. Additionally, organic hydrogen sulfides like sulfur-containing amino acids, dimethylsufoniopropinate and 2,3-dihydroxypropane-1 sulfonate are also highly present in surface waters and play vital roles in sulfur cycling (Hu et al. 2018). In natural respiration processes, Fe reduction precedes sulfate reduction. However, within our assay dichromate is a powerful oxidate and could be used to oxide reduced Fe and S, resulting in high $r_{\text{-}O2:C}$. Although this is still to be considered, [PCOD] is more constrained than [POC] throughout the time-series (Fig. 2), so if we are oxidizing either element, it is being done uniformly. Another caveat we recognize is the lack of sample blanking. Previously we touched upon the idea that sample blanking is not important for open ocean samples because of the high volume filtered (Moreno et al. 2022). Due to high biomass within coastal waters, the filtered volume within this study is smaller (300 mL compared to 2 L vs 8 L). The minimal variation in [PCOD], provides evidence that blanking would also not play a strong role in quantifying the $r_{\text{-}O2:C}$. Our third caveat is the presence of non-biological material (i.e., sand or dirt). During periods of higher biomass, darker filters are observed. High biomass filters can become packed or overloaded, allowing for higher rates of excess biological and non-biological material (including nanoparticles) present on filters. Note that darker filters are not equivalent to higher ratios. Although there are a few recognized caveats, our findings are bringing new insights into coastal variation and are robust.

5. Conclusions

Our study suggests that the $r_{\text{-}O2:C}$ is controlled by plankton's response to nutrient stressors. High $r_{\text{-}O2:C}$ along the coast has very strong implications on future hypoxic region expansions and general ecosystem health. Given future rising surface ocean temperatures (Durack et al. 2018; Kwiatkowski et al. 2020; Rasmussen et al. 2020) and continued changes to nutrients, $r_{\text{-}O2:C}$ dynamics further the complexities of coastal deoxygenation. Both direct (nutrient concentrations) and indirect (community shifts) controls play important roles in setting $r_{\text{-}O2:C}$ and therefore future oxygen levels. Although much research is needed to understand the mechanistic responses to nutrients and its effects on coastal oxygen levels, changes to community structure could be vital in a changing climate. Particularly if we consider the impact HABs could have on both the $r_{\text{-}O2:C}$ and deoxygenation events. *Pseudo-nitzschia* is a common HAB forming species found extensively along the California coast, producing domoic acid (DA) in a variety of concentrations (Lelong et al. 2012). DA induction can occur for a range of conditions but one of the leading accepted factors is nutrient limitation (Bates et al. 1991; Buck 1992; Garrison et al. 1992; Fehling et al. 2004, p. 20; Lelong et al. 2012). In 2017, we see an increase in the relative abundance of *Pseudo-nitzschia* sp. (Fig. 4B) which corresponds to an increased $r_{\text{-}O2:C}$. If increased temperatures stratify our coastlines, we expect to have an increase in HAB events (McCabe et al. 2016; Smith et al. 2018). Following many large-scale HAB events, there are declines in deep ocean oxygen levels killing off a portion of fish populations (Anderson et al. 2021). It has been observed both in field and laboratory experiments that the overall rate of oxygen produced by phytoplankton can change significantly as a result of increased temperature (Hancke and Glud 2004; Robinson 2019). With increased temperatures

https://doi.org/10.5194/egusphere-2025-2357
Preprint. Discussion started: 2 June 2025

leading to decreased nutrients, we may observe higher $r_{-O2:C}$ ratios and increased deoxygenation events along our coastline. Ultimately, the MICRO $r_{-O2:C}$ is higher than previously measured open ocean samples. Our findings have strong implications for future respiration and oxygen cycling.

Author contribution: ARM and ACM designed the time-series. ARM and AJF collected and analyzed samples. ARM prepared the manuscript with contributions and edits from all co-authors.

Competing interests: The authors declare that they have no conflict of interest.

Acknowledgements: We thank all undergraduate students through the years that participated at the MICRO time-series, as well as Alyse Larkin for their assistance in editing our manuscript.

Financial support: NSF GRFP, UCI Chancellor's Club Fellowship, and the UCLA Chancellor's Postdoctoral Fellowship to ARM as well as NSF OCE-2135035 and NSF-OCE 1948842 to ACM.

References:

Aktas DF, Lee JS, Little BJ, et al (2013) Effects of oxygen on biodegradation of fuels in a corroding environment. International Biodeterioration and Biodegradation 81:114–126. https://doi.org/10.1016/j.ibiod.2012.05.006

Anderson DM, Fensin E, Gobler CJ, et al (2021) Marine harmful algal blooms (HABs) in the United States: History, current status and future trends. Harmful Algae 102:101975. https://doi.org/10.1016/j.hal.2021.101975

Anderson LA (1995) On the hydrogen and oxygen content of marine phytoplankton. Deep Sea Research Part I: Oceanographic Research Papers 42:1675–1680. https://doi.org/10.1016/0967-0637(95)00072-E

Bates SS, de Freitas ASW, Milley JE, et al (1991) Controls on Domoic Acid Produciton by the Diatom *Nitzschia pungens f. multiseries* in Culture: Nutrients and Irradiance. Canadian Journal of Fisheries and Aquatic Sciences 48:1136–1144

Bograd SJ, Castro CG, Di Lorenzo E, et al (2008) Oxygen declines and the shoaling of the hypoxic boundary in the California Current. Geophysical Research Letters 35:1–6. https://doi.org/10.1029/2008GL034185

Buck KR (1992) Autecology of the diatom *Pseudonitzschia australis*, a domoic acid producer, from Monterey Bay, California. Marine Ecology Progress Series 84:293–302. https://doi.org/10.3354/meps084293

Durack PJ, Gleckler PJ, Purkey SG, et al (2018) Ocean Warming: From the Surface to the Deep in Observations and Models. Oceanography 31:41–51

Fagan AJ, Moreno AR, Martiny AC (2019) Role of ENSO Conditions on particulate organic matter concentrations and elemental ratios in the Southern California Bight. Frontiers in Marine Science 6:1–8. https://doi.org/10.3389/fmars.2019.00386

Falkowski PG, Algeo T, Codispoti L, et al (2011) Ocean Deoxygenation: Past, Present, and Future. Eos, Transactions American Geophysical Union 92:

https://doi.org/10.5194/egusphere-2025-2357
Preprint. Discussion started: 2 June 2025

Fehling J, Davidson K, Bolch CJ, Bates SS (2004) Growth and domoic acid production by P*seudo-nitzschia seriata* (Bacillariophyceae) under phosphate and silicate limitation. Journal of Phycology 40:674–683. https://doi.org/10.1111/j.1529-8817.2004.03213.x

Fuentes S, Barra B, Gregory Caporaso J, Seeger M (2016) From rare to dominant: A fine-tuned soil bacterial bloom during petroleum hydrocarbon bioremediation. Applied and Environmental Microbiology 82:888–896. https://doi.org/10.1128/AEM.02625-15

Garrison DL, Conrad SM, Eilers PP, Waldron EM (1992) Confirmation of Domoic Acid Production by *Pseudonitzschia Australis* (Bacillariophyceae) Cultures. J Phycol 28:604–607

Gerace SD, Fagan AJ, Primeau FW, et al (2023) Depth Variance of Organic Matter Respiration Stoichiometry in the Subtropical North Atlantic and the Implications for the Global Oxygen Cycle. Global Biogeochemical Cycles 37:e2023GB007814. https://doi.org/10.1029/2023GB007814

Hancke K, Glud RN (2004) Temperature effects on respiration and photosynthesis in three diatom-dominated benthic communities. Aquatic Microbial Ecology 37:265–281. https://doi.org/10.3354/ame037265

Hazen TC, Dubinsky EA, DeSantis TZ, et al (2010) Deep-Sea Oil Plume Enriches Indigenous Oil-Degrading Bacteria. Science 330:204–209

Homoky WB, Conway TM, John SG, et al (2021) Iron colloids dominate sedimentary supply to the ocean interior. Proceedings of the National Academy of Sciences of the United States of America 118:. https://doi.org/10.1073/PNAS.2016078118

Hu X, Liu J, Liu H, et al (2018) Sulfur metabolism by marine heterotrophic bacteria involved in sulfur cycling in the ocean. Science China Earth Sciences 61:1369–1378. https://doi.org/10.1007/s11430-017-9234-x

Hutchins DA, DiTullio GR, Zhang Y, Bruland KW (1998) An iron limitation mosaic in the California upwelling regime. Limnology & Oceanography 43:1037–1054. https://doi.org/10.4319/lo.1998.43.6.1037

Johnson KS, Chavez FP, Friederich GE (1999) Continental-Shelf sediment as a primary source of iron for coastal phytoplankton. Nature 398:697–700

Jones MN (1984) Nitrate reduction by shaking with cadmium. Alternative to cadmium columns. Water Research 18:643–646. https://doi.org/10.1016/0043-1354(84)90215-X

Juneja A, Ceballos RM, Murthy GS (2013) Effects of environmental factors and nutrient availability on the biochemical composition of algae for biofuels production: A review. Energies 6:4607–4638. https://doi.org/10.3390/en6094607

Karl DM, Tien G (1992) MAGIC: A sensitive and precise method for measuring dissolved phosphorus in aquatic environments. Limnology and Oceanography 37:105–116. https://doi.org/10.4319/lo.1992.37.1.0105

Keeling RE, Körtzinger A, Gruber N (2010) Ocean deoxygenation in a warming world. Annual review of marine science 2:199–229. https://doi.org/10.1146/annurev.marine.010908.163855

https://doi.org/10.5194/egusphere-2025-2357
Preprint. Discussion started: 2 June 2025

Knap A, Michaels A, Dow R, et al (1993) Bermuda Atlantic timeseries study methods manual (Version 3). Bermuda biological station for research. Inc, US JGOFS

Kondo Y, Moffett JW (2015) Iron redox cycling and subsurface offshore transport in the eastern tropical South Pacific oxygen minimum zone. Marine Chemistry 168:95–103. https://doi.org/10.1016/j.marchem.2014.11.007

Krachler R, Von Der Kammer F, Jirsa F, et al (2012) Nanoscale lignin particles as sources of dissolved iron to the ocean. Global Biogeochemical Cycles 26:1–9. https://doi.org/10.1029/2012GB004294

Kwiatkowski L, Torres O, Bopp L, et al (2020) Twenty-first century ocean warming, acidification, deoxygenation, and upper ocean nutrient decline from CMIP6 model projections. Biogeosciences Discussions 1–43. https://doi.org/10.5194/bg-2020-16

Lam PJ, Bishop JKB, Henning CC, et al (2006) Wintertime phytoplankton bloom in the subarctic Pacific supported by continental margin iron. Global Biogeochemical Cycles 20:1–12. https://doi.org/10.1029/2005GB002557

Larkin AA, Moreno AR, Fagan AJ, et al (2020) Persistent El Niño driven shifts in marine cyanobacteria populations. PLoS ONE 15:1–19. https://doi.org/10.1371/journal.pone.0238405

Leahy JG, Colwell RR (1990) Microbial degradation of hydrocarbons in the environment. Microbiological Reviews 54:305–315. https://doi.org/10.1128/mr.54.3.305-315.1990

Lelong A, Hégaret H, Soudant P, Bates SS (2012) *Pseudo-nitzschia* (Bacillariophyceae) species, domoic acid and amnesic shellfish poisoning: Revisiting previous paradigms. Phycologia 51:168–216. https://doi.org/10.2216/11-37.1

Lomas MW, Burke AL, Lomas DA, et al (2010) Sargasso Sea phosphorus biogeochemistry: an important role for dissolved organic phosphorus (DOP). Biogeosciences 7:695–710. https://doi.org/10.5194/bg-7-695-2010

Malmstrom RR, Coe A, Kettler GC, et al (2010) Temporal dynamics of *Prochlorococcus* ecotypes in the Atlantic and Pacific oceans. The ISME journal 4:1252–64. https://doi.org/10.1038/ismej.2010.60

Martiny AC, Talarmin A, Mouginot C, et al (2016) Biogeochemical interactions control a temporal succession in the elemental composition of marine communities. Limnology and Oceanography 61:531–542. https://doi.org/10.1002/lno.10233

Matear RJ, Hirst AC (2003) Long-term changes in dissolved oxygen concentrations in the ocean caused by protracted global warming. Global Biogeochemical Cycles 17:n/a--n/a. https://doi.org/10.1029/2002GB001997

McCabe RM, Hickey BM, Kudela RM, et al (2016) An unprecedented coastwide toxic algal bloom linked to anomalous ocean conditions. Geophysical Research Letters 43:10,366-10,376. https://doi.org/10.1002/2016GL070023

Moreno AR, Garcia CA, Larkin AA, et al (2020) Latitudinal gradient in the respiration quotient and the implications for ocean oxygen availability. Proceedings of the National Academy of Sciences 117:202004986. https://doi.org/10.1073/pnas.2004986117

https://doi.org/10.5194/egusphere-2025-2357
Preprint. Discussion started: 2 June 2025

539 Moreno AR, Larkin AA, Lee JA, et al (2022) Regulation of the Respiration Quotient Across Ocean
540 Basins. AGU Advances 3:1–12. https://doi.org/10.1029/2022AV000679

541 Nagarkar M, Countway PD, Du Yoo Y, et al (2018) Temporal dynamics of eukaryotic microbial diversity
542 at a coastal Pacific site. ISME Journal 12:2278–2291. https://doi.org/10.1038/s41396-018-0172-3

543 Pan XF, Yan BX, Muneoki Y (2011) Effects of land use and changes in cover on the transformation and
544 transportation of iron: A case study of the Sanjiang Plain, Northeast China. Science China Earth
545 Sciences 54:686–693. https://doi.org/10.1007/s11430-010-4082-0

546 Rasmussen LL, Carter ML, Flick RE, et al (2020) A Century of Southern California Coastal Ocean
547 Temperature Measurements. Journal of Geophysical Research: Oceans 125:1–11.
548 https://doi.org/10.1029/2019JC015673

549 Redfield AC (1958) The biological control of the chemical factors in the environment. American Scientist
550 46:1–18

551 Reitan KI, Rainuzzo JR, Olsen Y (1994) Effect of Nutrient Limitation of Fatty Acid and Lipid Content of
552 Marine Microalgae. J Phycol 30:972–979

553 Robinson C (2019) Microbial respiration, the engine of ocean deoxygenation. Frontiers in Marine Science
554 5:1–13. https://doi.org/10.3389/fmars.2018.00533

555 Schmidtko S, Stramma L, Visbeck M (2017) Decline in global oceanic oxygen content during the past
556 five decades. Nature 542:335–339. https://doi.org/10.1038/nature21399

557 Seubert EL, Gellene AG, Howard MDA, et al (2013) Seasonal and annual dynamics of harmful algae and
558 algal toxins revealed through weekly monitoring at two coastal ocean sites off southern
559 California, USA. Environmental Science and Pollution Research 20:6878–6895.
560 https://doi.org/10.1007/s11356-012-1420-0

561 Sharp JH (1974) Improved analysis for “particulate” organic carbon and nitrogen from seawater.
562 Limnology and Oceanography 19:984–989. https://doi.org/10.4319/lo.1974.19.6.0984

563 Smith J, Connell P, Evans RH, et al (2018) A decade and a half of *Pseudo-nitzschia* spp. and domoic acid
564 along the coast of southern California. Harmful Algae 79:87–104.
565 https://doi.org/10.1016/j.hal.2018.07.007

566 Tai V, Palenik B (2009) Temporal variation of *Synechococcus* clades at a coastal Pacific Ocean
567 monitoring site. The ISME journal 3:903–915. https://doi.org/10.1038/ismej.2009.35

568 Thompson PA, Guo M -x, Harrison PJ, Whyte JNC (1992) Effects of Variation in Temperature. I. on the
569 Fatty Acid Composition of Eight Species of Marine Phytoplankton. Journal of Phycology
570 28:488–497. https://doi.org/10.1111/j.0022-3646.1992.00488.x

571 Trainer VL, Pitcher GC, Reguera B, Smayda TJ (2010) The distribution and impacts of harmful algal
572 bloom species in eastern boundary upwelling systems. Progress in Oceanography 85:33–52.
573 https://doi.org/10.1016/j.pocean.2010.02.003

https://doi.org/10.5194/egusphere-2025-2357
Preprint. Discussion started: 2 June 2025

574 Varjani SJ, Gnansounou E (2017) Microbial dynamics in petroleum oilfields and their relationship with
575 physiological properties of petroleum oil reservoirs. Bioresource Technology 245:1258–1265.
576 https://doi.org/10.1016/j.biortech.2017.08.028

577 Venrick EL (2012) Phytoplankton in the California Current system off southern California: Changes in a
578 changing environment. Progress in Oceanography 104:46–58.
579 https://doi.org/10.1016/j.pocean.2012.05.005

580 Yang T, Nigro LM, Gutierrez T, et al (2014) Pulsed blooms and persistent oil-degrading bacterial
581 populations in the water column during and after the Deepwater Horizon blowout. Deep-Sea
582 Research Part II: Topical Studies in Oceanography 129:282–291.
583 https://doi.org/10.1016/j.dsr2.2014.01.014

584